Synthesis of thermally stable and low band gap poly(azomethine-urethane)s containing fluorene unit in the backbone

İsmet Kaya*,†, Ali Avcı*,, and Kevser Temizkan***

*Çanakkale Onsekiz Mart University, Faculty of Sciences and Arts, Department of Chemistry,
Polymer Synthesis and Analysis Lab., 17020, Çanakkale, Turkey
**Celal Bayar University, Faculty of Sciences and Arts, Department of Chemistry, 45040, Manisa, Turkey

Abstract−New poly(azomethine-urethane)s (PAMU)s were prepared to investigate the effects of different four diisocyanates on some physical properties such as thermal stability, optical and electrochemical properties. First, the fluorene Schiff base was synthesized as in the literature. Then, this Schiff base was converted to poly(azomethine-urethane) using diisocyanates (2,4-toluenediisocyanate, 1,4-phenylene diisocyanate, methylene-di-*p*-phenyl-diisocyanate, and hexamethylene-diisocyanate) via condensation reaction. Second, the structures of PAMUs were confirmed by FT-IR, NMR, and UV-Vis spectral analyses. Cyclic voltammetry (CV) was used to determine the electrochemical oxidation-reduction characteristics of (PAMU)s. The CV results of PAMUs compounds showed to have an electrochemical band gap below such as 2.0 eV. The PAMUs were characterized by TGA, DSC, SEM, SEC and AFM techniques. TGA analysis results of compounds showed considerable increasing of the thermal stability of polymers, because of finding of azomethine bond in the main chain.

Keywords: Poly(azomethine-urethane)s, Polyfluorene, Thermal Analysis, Cyclic Voltammetry, Band Gap

INTRODUCTION

Poly(fluorenes) (PFs) and fluorene-containing copolymers have attracted considerable attention due to their high luminescence efficiency, thermal stability, and low band gaps [1-4]. They have good electrochemical properties, as well as good film-forming properties, and high processability [5-7]. Different methods have been reported for preparing of PFs via oxidative polymerization [8], electro polymerization [9], and condensation reactions [10] in the presence of FeCl$_3$.

Polyazomethines, which contain -HC=N bonds in their structure, exhibit excellent thermal stability and many desirable properties such as high mechanical strength, electrical conductivity, paramagnetism, metal-chelating that make these kinds of polymers interesting particularly in materials science [11,12]. These polymers have been also investigated for the optoelectrical applications such as hole transport layer for organic light-emitting diode (OLED), non-linear optics (NLO) and photovoltaic cell [13-15]. The C=N linkages of polyazomethines are electron withdrawing group; thus, they can be used to tune the highest occupied molecular orbital (HOMO) and lowest unoccupied molecular orbital (LOMO) energy levels of the electron-rich conjugated polymers [16]. Also, the various derivatives of conjugated polymers such as poly(azomethine-urethane)s [17], poly(azomethine-ester)s [18] and poly(azomethine-ether)s [19,20] have been synthesized and reported in the literature.

Polyurethanes (PUs) are present in many aspects of modern life. They represent a class of polymers that have found a widespread use in the medical, automotive and industrial fields. Polyurethanes can be found in products such as furniture, coatings, adhesives, constructional materials, fibers, paints, and synthetic skins [21-23]. On the other hand, fluorene unit-containing polyurethanes, polyesters, and polyethers have attracted current interest for their utilities such as optical materials with both high refractive indexes and very low birefringence properties, mechanically strong materials with high thermal stabilities, etc [24]. Azomethine derivatives of polyurethanes were reported in literature and clarified their thermal stabilities and optical properties [25-27]. According to our knowledge, poly(azomethine-urethane)s containing fluorene unit have not been studied yet. This class of PAMUs, thus, still needs to be researched with new contributions.

For this reason, we first synthesized new poly(azomethine-urethane)s including fluorene ring in the main chain. Second, characterization studies investigated different diisocyanates effect on thermal stability, optical, and electrochemical properties. For this reason, the obtained materials were characterized using FT-IR, UV-Vis, NMR, and SEC analyses. TG-DTA technique was used to determine thermal properties of compounds. DSC analyses of the poly(azomethine-urethane)s were also performed to determine the glass transition temperatures (T_g). The HOMO-LUMO energy levels and electrochemical band gap values were obtained by using cyclic voltammetry (CV) measurements. Also, the fluorescence spectra of the poly(azomethine-urethane)s were carried out to determine

†To whom correspondence should be addressed.
E-mail: kayaismet@hotmail.com

the maximal emission-excitation intensities in DMF solution.

EXPERIMENTAL

1. Materials

2,4-Toluenediisocyanate (TDI), methylene di-p-phenyl diisocyanate (MDI), hexamethylene diisocyanate (HDI), 1,4-phenylene diisocyanate (PDI), were supplied from Aldrich Chemical Co (USA). 9,9-bis(4-aminophenyl)fluorene (FDA), 4-hydroxybenzaldehyde (4-HBA), dimethylformamide (DMF), dimethylsulfoxide (DMSO), tetrahydrofurane (THF), methanol, ethanol, acetonitrile, acetone, toluene, ethyl acetate, heptane, hexane, CCl_4, $CHCl_3$, H_2SO_4, KOH and HCl were supplied from Merck Chemical Co. (Germany) and used as received. 30% aqueous solution of sodium hypochlorite was supplied by Paksoy Chemical Co. (Turkey).

2. Synthesis of the FS

Fluorene Schiff base, abbreviated as FS, was synthesized by the condensation reaction of FDA with 4-hydroxybenzaldehyde (4-HBA). The reaction was performed as follows: FDA (1.74 g, 0.005 mol) was placed into a 250 mL three-necked round-bottom flask which was fitted with condenser, thermometer and magnetic stirrer. Fifty mL of methanol was added into the flask and reaction mixture was heated to 60 °C. A solution of 4-hydroxybenzaldehyde (1.22 g, 0.010 mol) in 20 mL methanol was added into the flask. Reactions were maintained for 3 h under reflux (Scheme 1). The product was filtered, recrystalled from acetonitrile and dried in a vacuum desiccator [28]. The yield of Schiff base compound was found as 74%.

^{1}H-NMR (DMSO-d6): 10.29 (s,-OH), 8.41 (s, -CH=N-), 7.88 (d, -Hi) 7.78, (d,-Hb), 7.49 (d, -He), 7.36 (m, -Hf, -Hg), 7.18 (d, -Hd), 7.12 (d,-Hc), 6.92 (d,-Ha). **^{13}C-NMR (DMSO-d6):** 163.86 (C1-ipso), 160.38 (C5-H), 151.06 (C6-ipso), 148.00 (C9-ipso), 143.11 (C11-ipso), 139.89 (C16-ipso), 132.62 (C3-H), 128.80 (C4-ipso), 128.15

(C12-H), 127.99 (C13-H), 121.35 (C14-H), 120.82 (C15-H), 116.37 (C7-H), 114.22 (C2-H), 64.80 (C10-ipso).
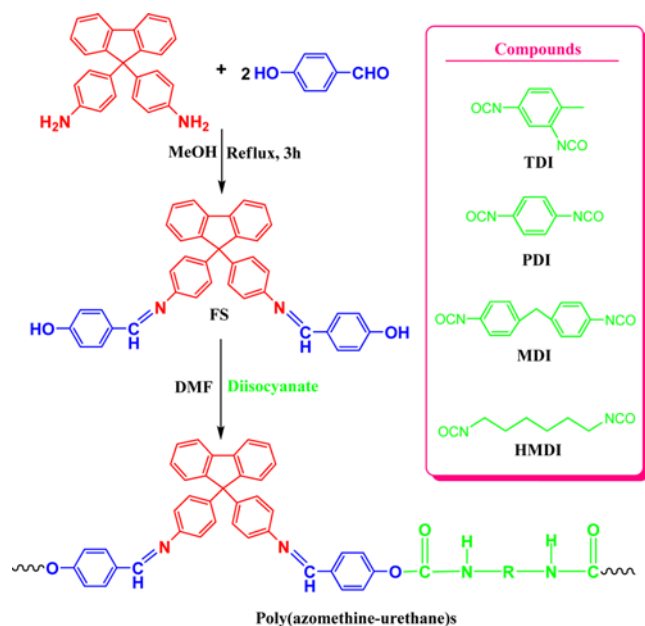
3. Syntheses of the PAMUs

Syntheses procedures of the PAMUs (FS-TDI, FS-PDI, FS-MDI, and FS-HMDI) were as follows: Diol monomer (0.01 mol) was dissolved in 30 mL dry DMF and added into a 250 mL three-necked round-bottom flask which was fitted with condenser, magnetic stirrer, and inert gas supplier. Reaction mixture was heated to 60 °C, and equivalent amounts of diisocyanates TDI (0.01 mol), PDI (0.01 mol), MDI (0.01 mol), and HMDI (0.01 mol) were dissolved in 30 mL DMF and added into the flask. Reactions were maintained for 6 h under argon atmosphere, cooled at room temperature, and kept for 24 h. The obtained PAMUs were washed by methanol (2×50 mL), acetonitrile (2×50 mL), and distilled water (2×50 mL) to remove the unreacted components [29]. The products were dried in a vacuum oven at 75 °C for 24 h. The yields of FS-TDI, FS-PDI, FS-MDI, and FS-HMDI were found as 85, 83, 86 and 88%, respectively. All the synthesis procedures of compounds are summarized in Scheme 1.

4. Characterization Techniques

The solubility tests were done in different solvents by using 1 mg sample and 1 mL solvent at 25 °C. The infrared and ultraviolet-visible spectra of compounds were recorded by PerkinElmer FT-IR Spectrum one and Analytikjena Specord 210 Plus, respectively. FT-IR spectra of the compounds were recorded on a KBr pellet by PerkinElmer FT-IR Spectrum one. ^{1}H and ^{13}C-NMR spectra of monomer and polymers (Bruker AC FT-NMR spectrometer operating at 400 and 100.6 MHz, respectively) were also recorded by using deuterated DMSO-d_6 as a solvent at 25 °C. Tetramethylsilane was used as an internal standard. Thermal data were obtained by using a PerkinElmer Diamond Thermal Analysis system. TG-DTA measurements were performed between 20-1,000 °C (in N_2, rate 10 °C/min). DSC analyses were carried out by using PerkinElmer Pyris Sapphire within the temperatures of 25-450 °C (in N_2, rate 10 °C/min). The number average molecular weight (M_n), weight average molecular weight (M_w) and polydispersity index (PDI) were determined by size exclusion chromatography (SEC) techniques of Shimadzu Co. For SEC investigations an SGX (100 Å and 7 nm diameter loading material) 3.3 mm i.d.×300 mm column, DMF (0.4 mL/min) as eluent and polystyrene standards were used with a refractive index detector (RID) to analyze the products at 25 °C. Topography and 3D images of the polymeric films were determined using atomic force microscopy (AFM) Alpha 300 A (WITec, Ulm, Germany). The films were prepared by spin coating technique onto glasses THF solutions of polymers. After the deposition of the polymeric layer on glass plates, the samples were thermally annealed for 2 hours at 60 °C under vacuum. Specified surface areas of polymers were scanned angularly by cantilever of non-contact mod (AC, 42 N/m, 285 kHz). Scanning electron microscopy (SEM) photographs of the polymers were recorded using a Philips XL-30S FEG-SEM instrument. Before morphological observation, the surface of samples was coated with a thin layer of gold using a sputter coater prior to microscopy.

5. Optical and Electrochemical Properties

Ultraviolet-visible (UV-Vis) spectra of compounds were measured by Analytik Jena Specord 210 Plus. The absorption spectra of

Scheme 1. Syntheses of gluorene schiff base and poly(azomethine-urethane)s.

compounds were recorded by using DMSO as a solvent at 25 °C. The optical band gaps (E_g) of compounds were calculated from their absorption edges. Cyclic voltammetry (CV) measurements were carried out with a CHI 660 C Electrochemical Analyzer (CH Instruments, Texas, USA) at a potential scan rate of 20 mV/s. All the experiments were performed in a dry box filled with argon at room temperature. The electrochemical potential of Ag was calibrated with respect to the ferrocene/ferrocenium (Fc/Fc$^+$) couple. The half-wave potential ($E^{1/2}$) of (Fc/Fc$^+$) measured in acetonitrile solution of 0.1 M tetrabutylammonium hexafluorophosphate (TBAPF$_6$) and was 0.39 V with respect to Ag wire. The voltammetric measurements were carried out in acetonitrile and acetonitrile/DMSO mixture (v/v : 5/1) for the Schiff bases and the polymers, respectively. The HOMO-LUMO energy levels and electrochemical band gaps (E'_g) were calculated from oxidation and reduction peak potentials [30].

6. Fluorescence Measurements

A Shimadzu RF-5301PC spectrofluorophotometer was used in fluorescence measurements. Emission and excitation spectra of the synthesized compounds were obtained in solution forms in DMF for the polymers. Measurements were made in a wide concentration range between 2.5 and 40 mg/mL to determine the optimal fluorescence concentrations. Slit width in all measurements was 5 nm.

RESULTS AND DISCUSSION

1. Solubilities of the Compounds

The solubility test results of poly(azomethine-urethane)s are shown in Table 1, indicating that all the synthesized compounds are soluble in highly polar solvents such as DMSO, DMF, and NMP, while they are insoluble in acetone, methanol, and hexane. Additionally, they are partly soluble in THF. As a result, solubilities of synthesized polymers were limited because of their high molecular weight and intermolecular hydrogen-bonding.

2. Structures of the Compounds

FTIR spectra of the starting materials synthesized compounds are given in Fig. 1(a) and (b). According to Fig. 1(a), characteristic aldehyde and hydroxyl (-OH) peaks of 4-dihydroxy benzaldehyde (4-HBA) are observed at 1,688 and 3,164 cm^{-1}, respectively. At the FT-IR spectra of FDA, -NH$_2$ peaks are observed at between 3,432-3,345 cm^{-1}. The structure of the synthesized FS is confirmed by growing imine (-CH=N) peak with disappearing of the -NH$_2$ peak at PDA and the carbonyl (-C=O) peak of 4-HBA used in the condensation reaction. At the FT-IR spectra of FS, imine (-CH=N) and hydroxyl (-OH) peaks are observed at 1,658 and 3,173 cm^{-1}, respectively. According to Fig. 1(b), hydroxyl (-OH) group at Schiff
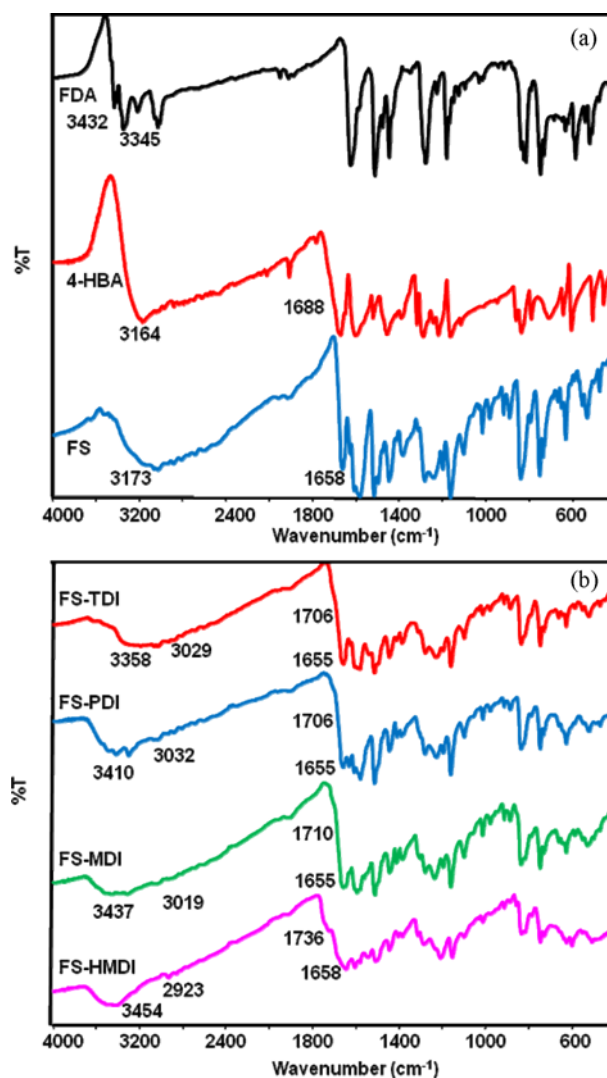

Fig. 1. FTIR spectra of starting materials and FS (a) and poly(azomethine-urethane)s (b).

base, and -C=O, -C=N stretch vibrations of diisocyanates disappear due to urethane formation. Moreover, at the FT-IR spectra of FS-TDI, FS-PDI, FS-MDI, FS-HMDI the new peaks appear between 3,358-3,454 and 1,706-1,736 cm^{-1}, respectively, which could be attributed to urethane -NH and carbonyl (-C=O) stretch vibrations, respectively. The peaks of carbonyl groups of poly(azomethine-urethane)s are observed as a narrow shoulder [25]. Azomethine bonds

Table 1. Solubility test results of poly(azomethine-urethane)s

Compounds	DMSO	DMF	NMP	THF	Acetone	MeOH	n-Hexane
FS	+	+	+	±	−	−	−
FS-TDI	+	+	+	±	−	−	−
FS-PDI	+	+	+	±	−	−	−
FS-MDI	+	+	+	±	−	−	−
FS-HMDI	+	+	+	±	−	−	−

+ Soluble, Partially soluble, − Insoluble

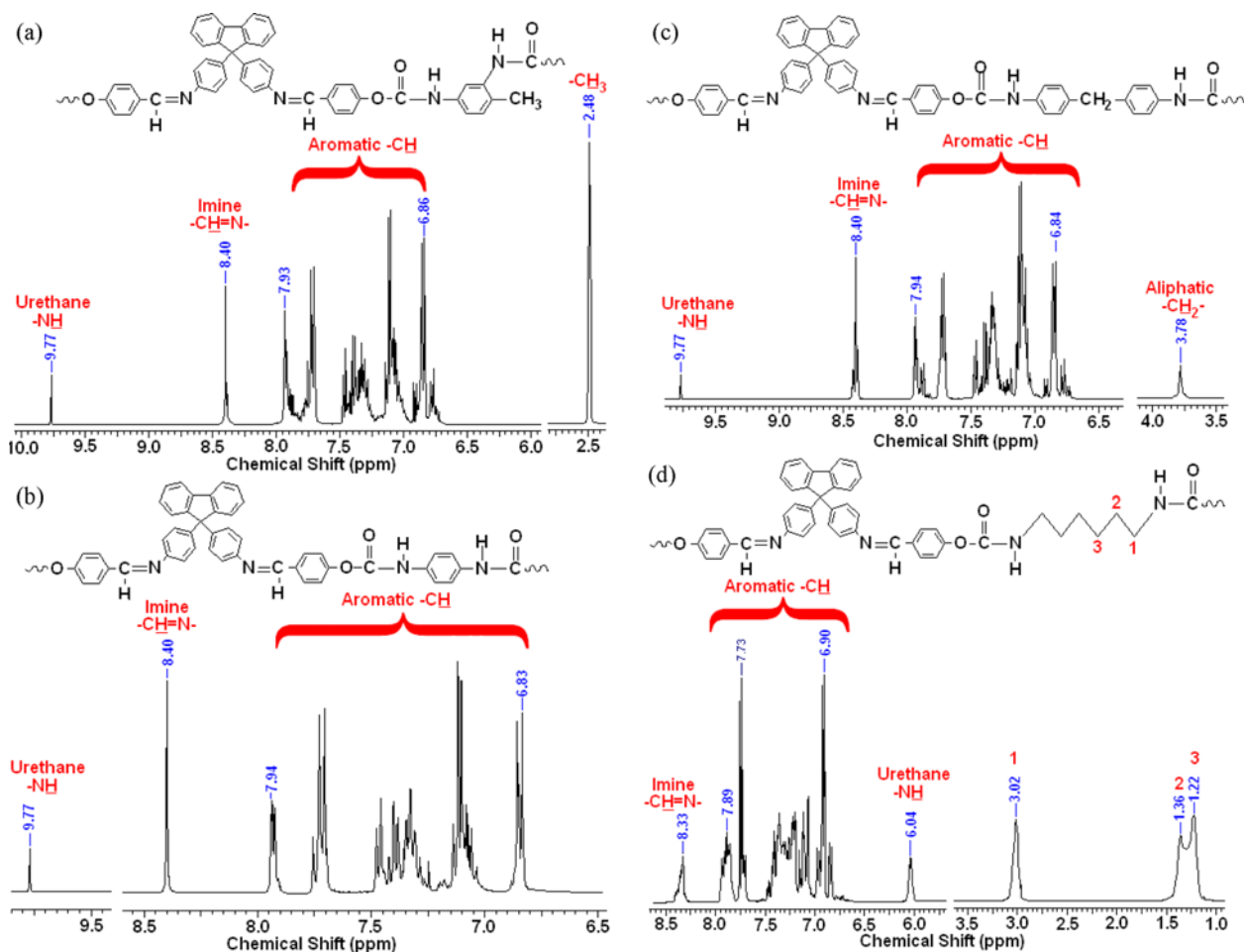**Fig. 2.** ^{1}H NMR spectra of FS-TDI (a), FS-PDI (b), FS-MDI (c) and FS-HMDI (d).

(-N=CH) in the structures of the PAMUs are observed between 1,655 and 1,658 cm^{-1}. The observed results clearly confirm the formation of poly(azomethine-urethane)s [25,26].

^{1}H-NMR spectra of poly(azomethine-urethane)s are also given in Figs. 2(a), 2(b), 2(c), and 2(d). According to these figures, urethane (-NHCO) and imine (-CH=N) protons of FS-TDI, FS-PDI and FS-MDI are observed at 9.77 ppm [25] and 8.40 ppm, respectively. At the spectra of FS-HMDI, the same peaks are observed 6.04 ppm [27] and 8.33 ppm, respectively. Aromatic ring protons are observed between 6.83-7.94 ppm for all synthesized polymers. Methyl (-CH₃) protons of FS-TDI and aliphatic -CH₂- protons of FS-MDI are observed 2.48 ppm and 3.78 ppm, respectively. Also aliphatic protons of FS-HMDI are observed between 1.22-3.02 ppm. NMR analyses results indicate the formation of polymers [25-31].

3. Size Exclusion Chromatography

According to the SEC chromatograms, the calculated number average molecular weight (M_n), weight average molecular weight (M_w), and polydispersity index (PDI) values of FS-TDI, FS-PDI, FS-MDI, and FS-HMDI were measured using an RI detector. According to the SEC results, the M_n values of FS-TDI, FS-PDI, FS-MDI, and FS-HMDI were calculated as 12,250, 19,600, 7,400, and 11,900 g mol^{-1}, respectively. The M_w values of FS-TDI, FS-PDI, FS-MDI, and FS-HMDI were calculated as 16,500, 25,400, 13,200 and

17,350 g mol^{-1}, respectively. Also, PDI values of FS-TDI, FS-PDI, FS-MDI, and FS-HMDI were determined as 1.347, 1.296, 1.784 and 1.458, respectively. According to the total values of average molecular weight, FS-TDI, FS-PDI, FS-MDI and FS-HMDI had nearly 17-23, 28-36, 9-17 and 17-24 repeated units.

4. Fluorescence Characteristics

Fluorescence characteristics of the synthesized poly(azomethine-urethane)s were determined using DMF solutions at different concentrations [32]. Also, the optimization of the concentrations to obtain maximal emission intensity was investigated in DMF. Because all the poly(azomethine-urethane)s are completely soluble in DMF, it is chosen as solute. Figs. 3-6 show the excitation and emission spectra of FS-TDI, FS-PDI, FS-MDI, and FS-HMDI, respectively. The obtained results are also summarized in Table 2. These figures also indicate the concentration-fluorescence intensity relationships of the compounds. As seen in Figs. 3-6 and Table 2, the optimum concentration to obtain maximal emission-excitation intensities changes between 20 and 5 mg/mL. According to these the results, the order of the fluorescence intensities of the poly(azomethine-urethane)s is different and they changed as follows: FS-MDI <FS-PDI<FS-HMDI<FS-TDI. According to Table 2, FS-TDI has highest fluorescence intensity. This could probably be from the effect of methyl group in the structure of FS-TDI.
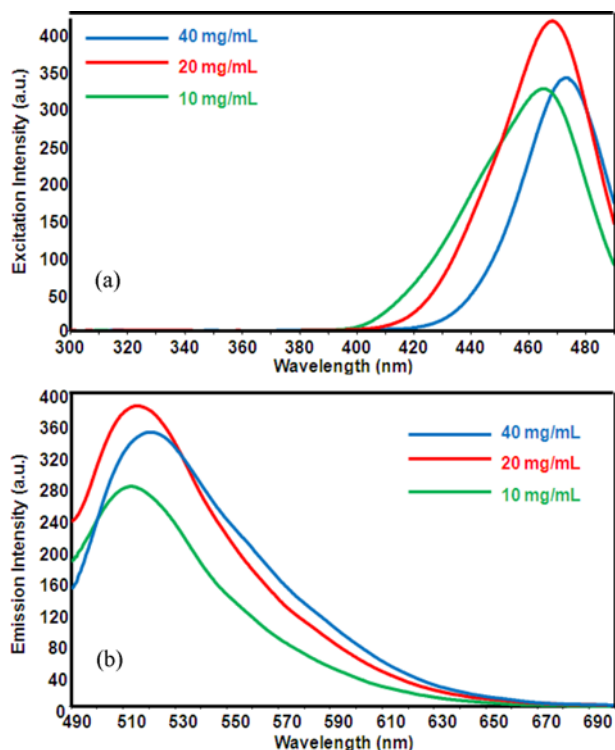
Fig. 3. Excitation (a) and emission (b) spectra of various concentrated solutions of FS-TDI in DMF.
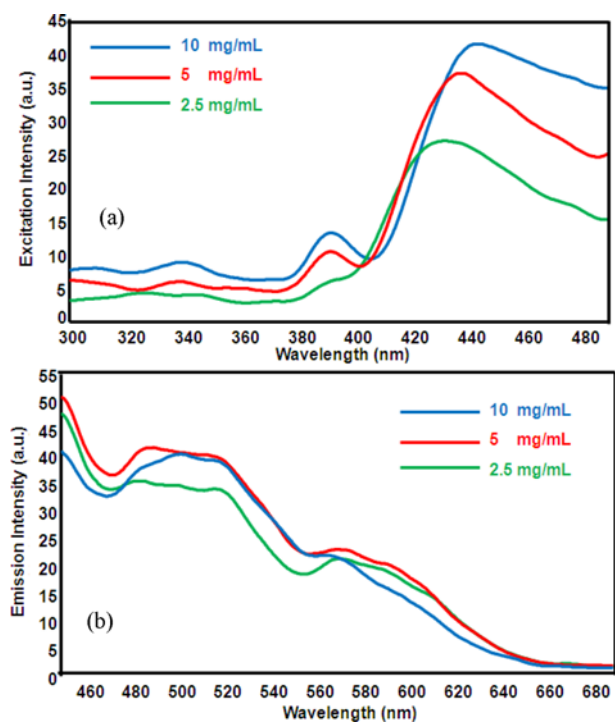

Fig. 4. Excitation (a) and emission (b) spectra of various concentrated solutions of FS-PDI in DMF.
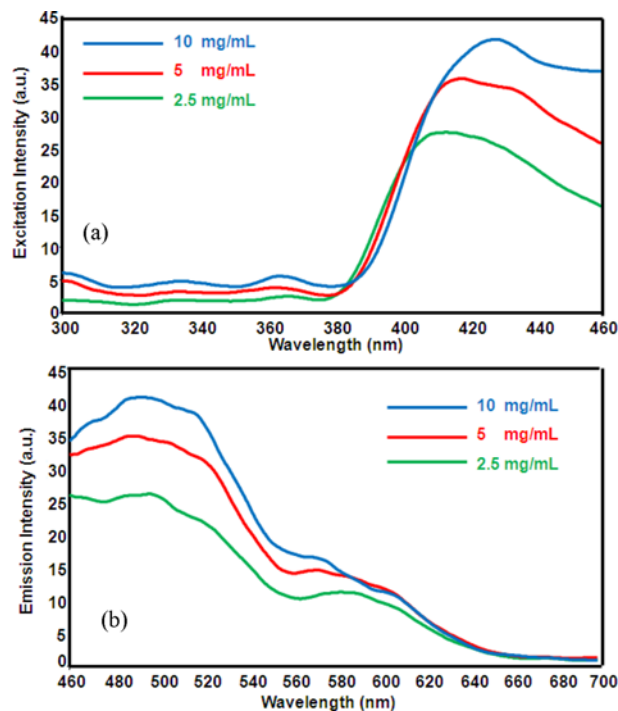

Fig. 5. Excitation (a) and emission (b) spectra of various concentrated solutions of FS-MDI in DMF.

Fig. 6. Excitation (a) and emission (b) spectra of various concentrated solutions of FS-HMDI in DMF.

5. Optical and Electrochemical Properties

According to UV-vis spectra, the absorption peaks of poly(azomethine-urethane)s appeared between 280-290 nm, due to the ure-thane group in the structure. Also, $\pi \rightarrow \pi^*$ transition peaks of the compounds were observed between 320-334 nm, respectively, due to azomethine linkage in the structure [33].
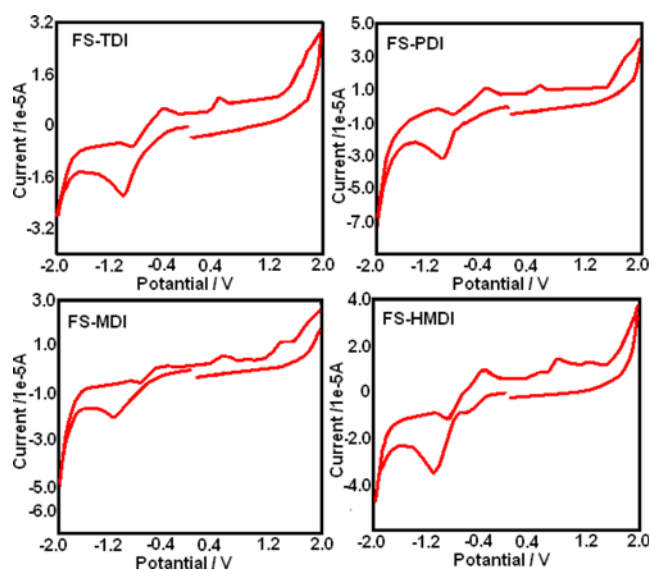
The cyclic voltammograms of synthesized poly(azomethine-ure-

Table 2. Fluorescence spectral data of the synthesized poly(azomethine-urethane)s

Compound	Conc (mg/mL)	$\lambda_{Ex}{}^{a}$	$\lambda_{Em}{}^{b}$	$\lambda_{max(Ex)}{}^{c}$	$\lambda_{max(Em)}{}^{d}$	$I_{Ex}{}^{e}$	$I_{Em}{}^{f}$	$\Delta\lambda_{ST}{}^{g}$
FS-TDI	20	475	520	468	516	416	383	48
FS-HMDI	10	430	510	426	512	60	59	86
FS-MDI	5	430	500	428	493	41	41	65
FS-PDI	5	430	530	438	489	37	42	51

[a]Excitation wavelength for emission
[b]Emission wavelength for excitation
[c]Maximum excitation wavelength
[d]Maximum emission wavelength
[e]Maximum excitation intensity
[f]Maximum emission intensity
[g]Stoke's shift

thane)s are given in Fig. 7. The HOMO-LUMO energy levels and the electrochemical band gaps (E'_g) poly(azomethine-urethane)s were calculated from the cyclic voltammetry (CV) measurements, and also these data given in Table 3. These data were estimated by using the oxidation onset (E_{ox}) and reduction onset (E_{red}) values.

Fig. 7. Cyclic voltammograms of the synthesized of poly(azomethine-urethane)s.

Table 3. Electronic structure parameters of the synthesized poly(azomethine-urethane)s

Compounds	HOMO (eV)[b]	LUMO (eV)[b]	E'_g (eV)[c]
FS	−5.42	−2.60	2.82
FS-TDI	−4.84	−3.39	1.44
FS-PDI	−4.85	−3.39	1.45
FS-MDI	−5.75	−3.25	2.50
FS-HMDI	−5.16	−3.31	1.86

[a]Highest occupied molecular orbital
[b]Lowest unoccupied molecular orbital
[c]Electrochemical band gap

The calculations were made by using the following equations [30]:

$$E_{HOMO}=-(4.39+E_{ox}) \tag{1}$$

$$E_{LUMO}=-(4.39+E_{red}) \tag{2}$$

$$E'_g=E_{LUMO}-E_{HOMO} \tag{3}$$

In our previous study, electrochemical band gap of FS was calculated as 2.82 eV [28]. As seen in Table 3, the order of electrochemical band gaps (E'_g) is as follows: FS>FS-MDI>FS-HMDI>FS-PDI>FS-TDI. Obtained results indicate that after the step-growth polymerization reactions, HOMO energy levels increase while LUMO energy levels decrease, and so the electrochemical band gaps (E'_g) of the poly(azomethine-urethane)s are lower than the Schiff base monomer. Lower band gaps facilitate the electronic transitions between HOMO-LUMO energy levels and make the poly(azomethine-urethane)s more electro-conductive than the monomers. As seen in Table 3, the synthesized FS-TDI and FS-PDI have below 1.5 eV electrochemical band gap. Therefore, they can be successfully applied in heterojunction solar cells [33].
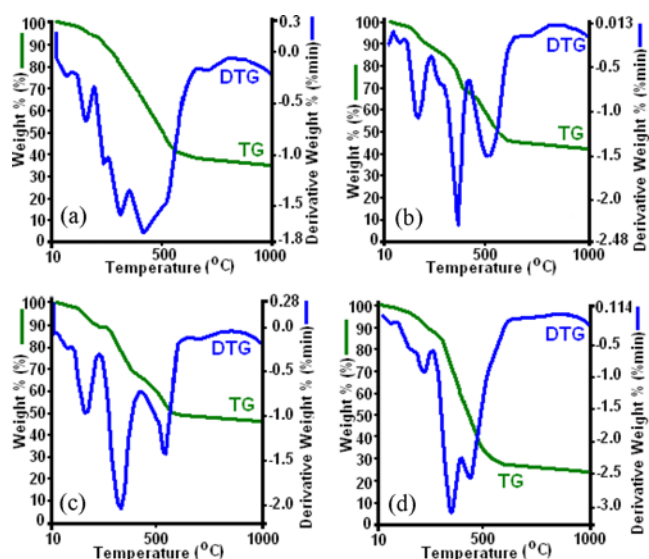

Fig. 8. TG-DTG curves of FS-TDI (a), FS-PDI (b), FS-MDI (c), and FS-HMDI (d).

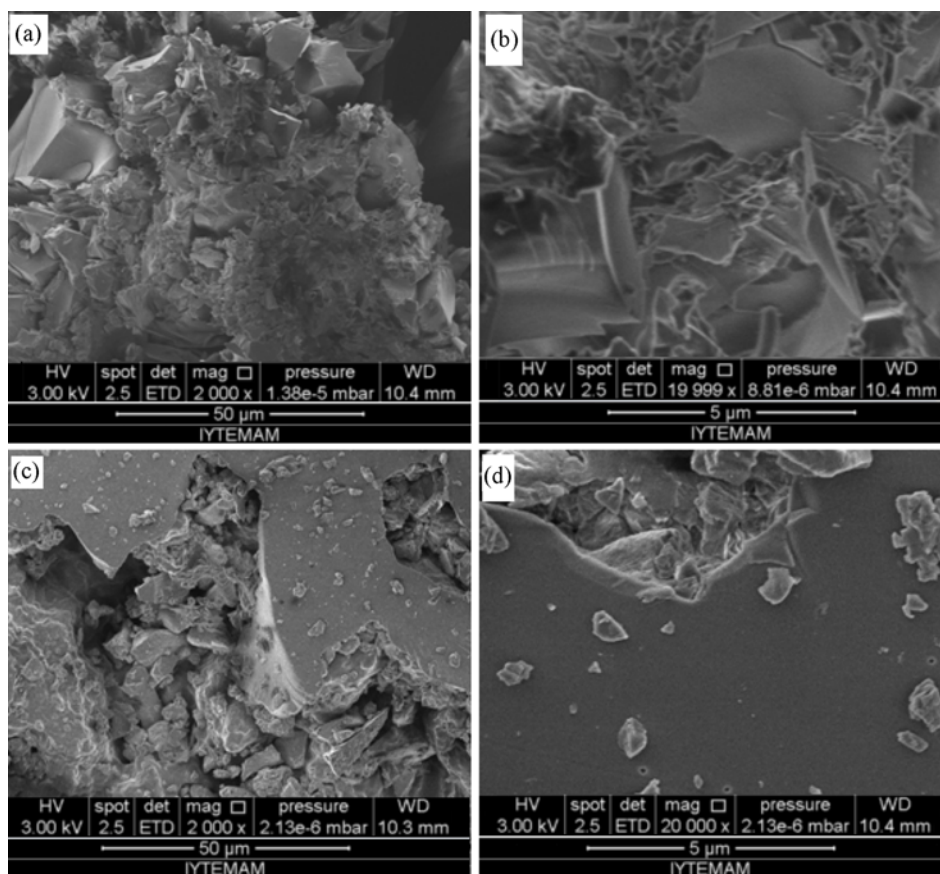**Table 4. Thermal degradation values of the synthesized pol(azomethine-urethane)s**

Compounds	T_{on} (^{o}C)[a]	W_{max} T (^{o}C)[b]	20% Weight losses	50% Weight losses	% Char at 1,000 ^{o}C	DTA Exo/Endo	DSC Tg (^{o}C)[c]	ΔCp (J/g^{o}C)[d]
FS-TDI	218	166,248,319,424	337	521	36	247,601 / 479	130	0.329
FS-PDI	337	176,368,515	356	580	44	192,364,848 / 622	136	0.365
FS-MDI	291	170,331,543	334	728	48	576 / 187,304	129	0.368
FS-HMDI	308	225,354,438	334	441	26	587 / 228,486	133	0.286

[a]The onset temperature

[b]Maximum weight loss temperature

[c]Glass transition temperature

[d]Change of specific heat during glass transition

6. Thermal Analyses

Thermal degradation properties of the fluorene containing poly (azomethine-urethane)s were determined by TG-DTG technique. TG-DTG curves of FS-TDI, FS-PDI, FS-MDI, and FS-HMDI are shown in Fig. 8, and the obtained results are also summarized in Table 4. 2-3% weight losses between 10-110 ^{o}C are attributed to losses of moisture or solvent [25,26,33]. According to DTA analysis, endothermic and exothermic peaks were observed depending on the heat exchange of substance at the places where there was a thermal degradation. According to the DTG curves FS-PDI, FS-MDI, and FS-HMDI thermally degrade in main three steps, while FS-TDI degrades in main four steps. According to Table 4, the onset temperature (T_{on}) of the obtained poly(azomethine-urethane)s was measured between 218 and 337 ^{o}C. According to TG results, FS-TDI, FS-PDI, and FS-MDI have higher char than FS-HMDI. T_{20} and T_{50} of poly(azomethine-urethane)s analysis, FS-MDI has the highest thermal stability. TGA data indicate that FS-MDI exhibits good thermal stability compared with other poly(azomethine-urethane)s because of an increase in the phenyl rings of MDI [34]. This variation in weight loss was due to the differences in the structure of hard segments of PAMUs. As seen in Scheme 1, FS-TDI, FS-PDI, and FS-MDI were synthesized aromatic diisocyanates, while FS-HMDI was synthesized aliphatic diisocyanate. As known, aromatic compounds have higher thermal stability than aliphatic

Fig. 9. SEM photographs of FS-TDI (a) and (b), FS-PDI (c) and (d), FS-MDI (e) and (f), and FS-HMDI (g) and (h).
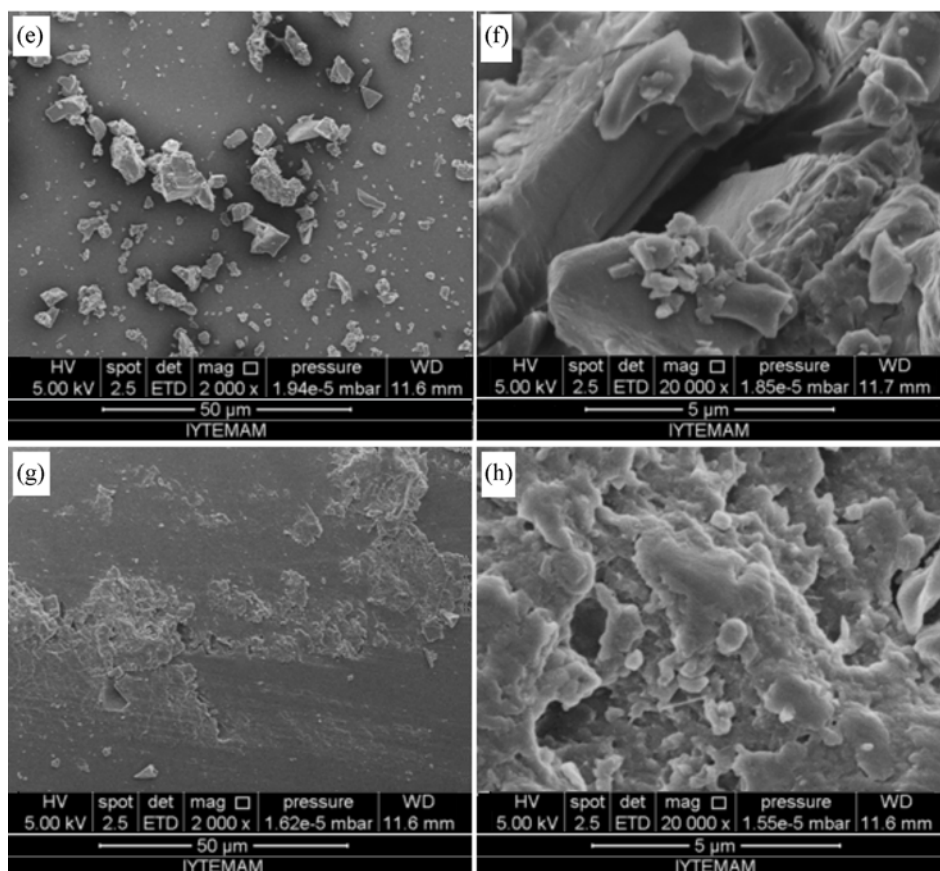
Fig. 9. Continued.

compounds [35].

The obtained results from DSC traces are also summarized in Table 3. According to the DSC curves the glass transition temperatures (T_g) are calculated as 130, 136, 129, and 133 °C for FS-TDI, FS-PDI, FS-MDI, and FS-HMDI, respectively. According to these results, the glass transition temperature (T_g) value of FS-PDI was the highest than other polymers. Also, the changes of the specific heats (ΔC_p) during the glass transitions are calculated from DSC measurements. The ΔC_p values of FS-TDI, FS-PDI, FS-MDI, and FS-HMDI are calculated as 0.329, 0.365, 0.368, and 0.286 J/g K, respectively.

7. Scanning Electron Microscopy

Morphological properties of the synthesized polymers are ob-tained by scanning electron microscopy (SEM). SEM photographs of powder forms of polymers are given in Fig. 9, which shows SEM photographs of polymers at different particle sizes. According to SEM photographs, aromatic diisocyanates derived polymers have more acutely particle structure. Aliphatic diisocyanate based FS-HMDI has smooth structure. This difference is attributable to the variations in molecular structures.

8. Atomic Force Microscopy

The AFM topography and 3D images of FS-MDI, FS-HMDI, FS-PDI and FS-TDI are given in Fig. 10. Here the compact particle structures of polymers are seen to be partly spherical, dispersed and unhomogeneous. The base particles look like ellipsoid shape, as shown in Fig. 10(b).
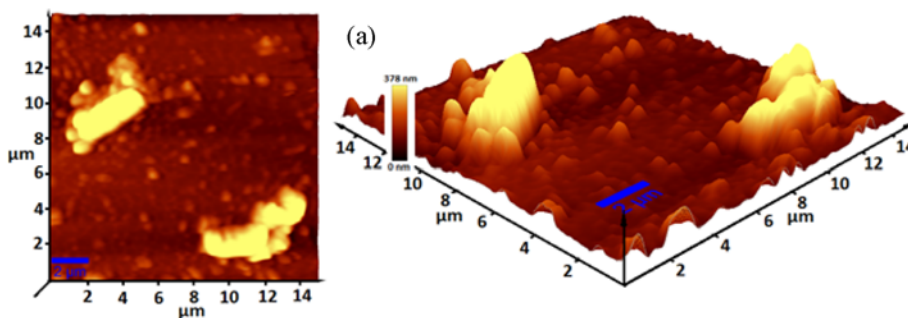

Fig. 10. AFM images of FS-MDI (a), FS-HMDI (b), FS-PDI (c) and FS-TDI (d).
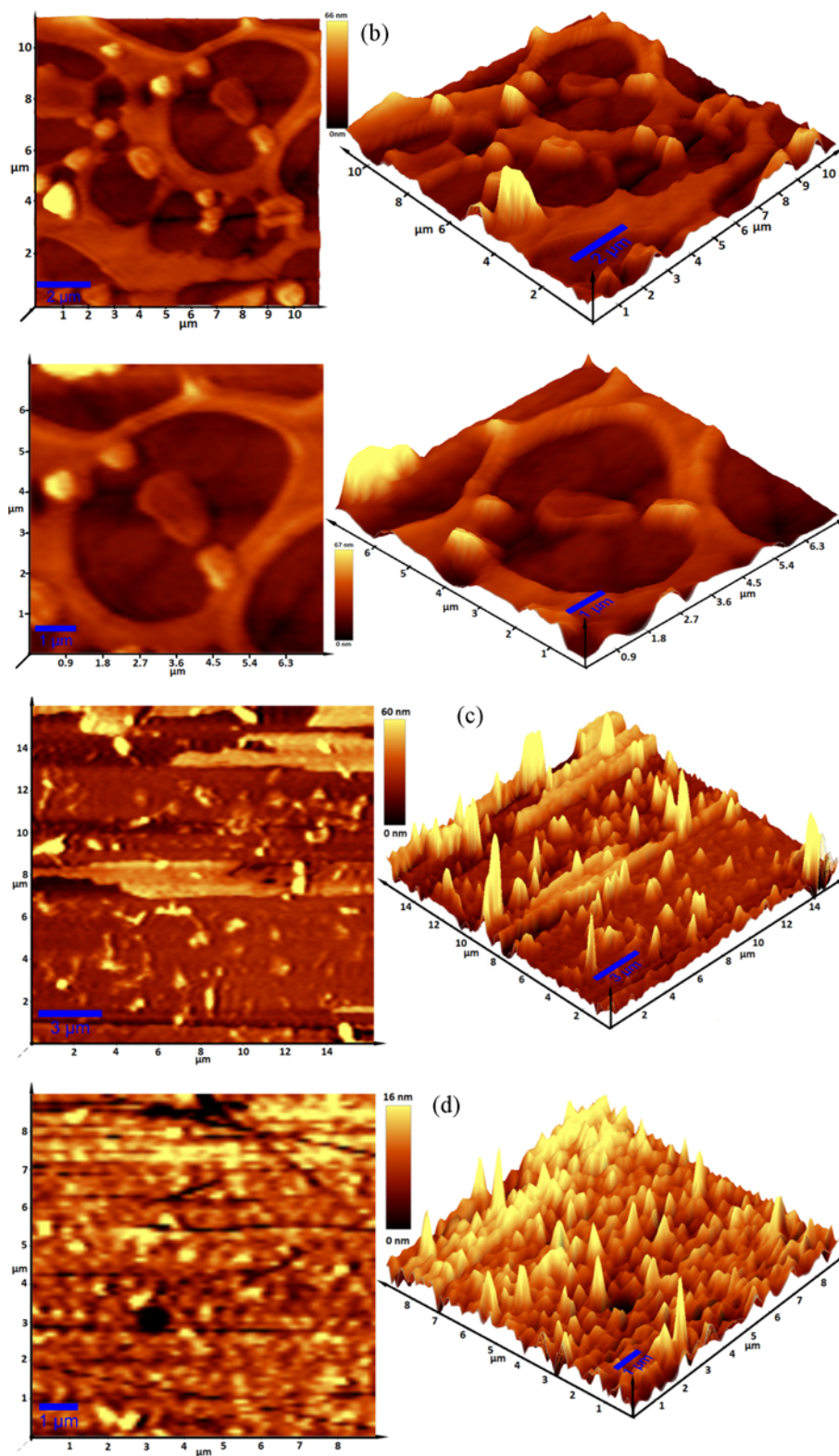
Fig. 10. Continued.

CONCLUSIONS

The novel fluorene-ring containing and thermally stable poly(azomethine-urethane)s were synthesized by step-growth polymeriza-tion reaction. Photoluminescence (PL) spectra of the synthesized compounds were obtained in DMF. According to fluorescence spectral data, FS-TDI has the highest excitation and emission intensity in DMF. According to CV results of the PAMUs, FS-TDI, FS-PDI,

and FS-HMDI have electrochemical band gap below 2.0 eV. Therefore, they can be successfully applied in heterojunction solar cells. Also, thermal analysis results showed that the synthesized polymers have high thermal stability. They have onset temperature between 218-337 °C and char above 26% at 1,000 °C. According to the DSC results, the synthesized PAMUs have Tg between 129 and 136 °C. As a result of the thermal analysis, FS-MDI has the highest thermal stability. Consequently, because of the fine thermal properties they can be promising candidates for aerospace applications.

REFERENCES

1. R. Tang, Z. Tan, Y. Li and F. Xi, *Chem. Mater.*, **18**, 1053 (2006).

2. A. Donat-Bouillud, I. Lévesgue, Y. Tao, M. D'Iorio, S. Beaupré, J. Bouchard and M. Leclerc, *Chem. Mater.*, **12**, 1931 (2000).

3. M. Leclerc, *J. Polym. Sci. Part A: Polym. Chem.*, **39**, 2867 (2001).

4. M. Francisco and M. Ricardo, *Adv. Funct. Mater.*, **17**, 71 (2007).

5. T. Ye, M. Zhu, J. Chen, Q. Fu, F. Zhao, C. Shi, Y. Hu, D. Ma and C. Yang, *J. Mater. Chem.*, **22**, 6413 (2012).

6. L. Ye, Z. K. Chen and T. L. Ye, *Polymer*, **51**, 1270 (2010).

7. J. Liu, J. Cao, S. Shao, Z. Xie, Y. Cheng, Y. Geng, L. Wang, X. Jing and F. Wang, *J. Mater. Chem.*, **18**, 1659 (2008).

8. M. Fukuda, K. Sawada, S. Morita and K. Yoshino, *Synth. Met.*, **41**, 855 (1991).

9. B. Dong, D. Song, L. Zheng, J. Xu and N. Li, *J. Electroanal. Chem.*, **633**, 63 (2009).

10. H. C. Kim, J. S. Kim, K. S. Kim, H. K. Park, S. Baek and M. Ree, *J. Polym. Sci. Part A: Polym. Chem.*, **42**, 825 (2004).

11. İ. Kaya and M. Yıldırım, *J. Appl. Polym. Sci.*, **110**, 539 (2008).

12. C. J. Yang and S. A. Jenekhe, *Chem. Mater.*, **6**, 196 (1994).

13. F. C. Tsai, C. C. Chang, C. L. Liu, W. C. Chen and S. A. Jenekhe, *Macromolecules*, **38**, 1958 (2005).

14. L. Ma, J. Cai, P. Zhao, H. Niu, C. Wang, X. Bai and W. Wang, *Mater. Chem. Phys.*, **133**, 333 (2012).

15. J. Weszka, M. Domanski, B. Jarzabek, J. Jurusik, J. Cisowski and A. Burian, *Thin Solid Films*, **516**, 3098 (2008).

16. J. C. Chen, Y. C. Liu, J. J. Ju, C. J. Chiang and Y. T. Chern, *Polymer*, **52**, 954 (2011).

17. İ. Kaya and M. Kamacı, *Prog. Org. Coat.*, **74**, 204 (2012).

18. L. Ravikumar, M. B. Prasad, B. J. Vasanthi, K. Gopalakrishnan, J. Rajeshkumar and V. Sengodan, *Mater. Chem. Phys.*, **115**, 632 (2009).

19. H. J. Yen and G. S. Liou, *Org. Electron.*, **11**, 299 (2010).

20. İ. Kaya, A. Avcı, F. Kolcu and S. Çulhaoğlu, *Des. Monomers Polym.*, **17**, 481 (2014).

21. D. K. Chattopadyay and D. C. Webster, *Prog. Polym. Sci.*, **34**, 1068 (2009).

22. D. K. Chattopadhyay and K. V. S. N. Raju, *Prog. Polym. Sci.*, **32**, 352 (2007).

23. T. Choi, K. A. Masser, E. Moore, J. Weksler, A. Padsalgikar and J. Runt, *J. Polym. Sci. Polym. Phys.*, **49**, 865 (2011).

24. K. Hiroki, Y. Ichikawa, H. Yamashita and J. Sugiyama, *Macromol. Rapid Commun.*, **29**, 809 (2008).

25. İ. Kaya, M. Yıldırım, M. Kamacı and A. Avcı, *J. Appl. Polym. Sci.*, **120**, 3027 (2011).

26. İ. Kaya and A. Avcı, *Mater. Chem. Phys.*, **133**, 269 (2012).

27. İ. Kaya and M. Kamacı, *J. Appl. Polym. Sci.*, **125**, 876 (2012).

28. İ. Kaya, M. Yıldırım, A. Aydın and D. Şenol, *React. Funct. Polym.*, **70**, 815 (2010).

29. İ. Kaya and A. Avcı, *J. Polym. Res.*, **19**, 9780 (2012).

30. İ. Kaya, M. Yıldırım and A. Avcı, *Synth. Met.*, **160**, 911 (2010).

31. İ. Kaya, M. Yıldırım, A. Avcı and M. Kamacı, *Macromolecular Research*, **19**, 286 (2011).

32. İ. Kaya, A. Avcı and Ö. Gültekin, *Chinese J. Polym. Sci.*, **30**, 796 (2012).

33. İ. Kaya and M. Kamacı, *J. Inorg. Organomet. Polym. Mater.*, **23**, 1159 (2013).

34. D. P. Suhas, H. M. Jeong, T. M. Aminabhavi and A. V. Raghu, *Polym. Eng. Sci.*, **54**, 24 (2014).

35. İ. Kaya and S. Uysal, *J. Appl. Polym. Sci.*, **120**, 3325 (2011).